X-621-69-57
PREPRINT

NASA TM X-63512

DIRECT MEASUREMENTS OF THE SIZE AND AMPLITUDE OF IRREGULARITIES IN THE TOPSIDE IONOSPHERE

P. L. DYSON

FEBRUARY 1969

GODDARD SPACE FLIGHT CENTER
GREENBELT, MARYLAND

X-621-69-57
PREPRINT

DIRECT MEASUREMENTS OF THE SIZE AND AMPLITUDE OF IRREGULARITIES IN THE TOPSIDE IONOSPHERE

by

P. L. Dyson

Goddard Space Flight Center
Greenbelt, Maryland

CONTENTS

DIRECT MEASUREMENTS OF THE SIZE AND AMPLITUDE OF IRREGULARITIES IN THE TOPSIDE IONOSPHERE

by

P. L. Dyson

ABSTRACT

Data obtained from the Alouette II Langmuir probe experiment during a 3-month period in the fall of 1966 have been examined for effects due to electron density irregularities (fine structure). Irregularities occur in patches hundreds of kilometers in horizontal extent, and individual irregularities have amplitudes between 5% (limit of resolution) and 70% and dimensions of less than 2 km along the satellite path. These irregularities appear more often at night than during the day and they occur in a region which is centered on the auroral oval and extends to both higher and lower latitudes. Comparison of the probe data with Alouette II ionograms obtained simultaneously shows that spread F occurred at the height of the satellite whenever fine structure was observed. However, particularly at mid latitudes, spread F often occurs at the satellite even when the probe does not detect irregularities. When spread F occurs, but the probe does not observe fine structure, the irregularities are less than 5% in amplitude (i.e. below the probe's resolution). Calculations using an irregularity model indicate that spread F is often caused by irregularities less than 0.5 km thick. Several irregularity production mechanisms which could account for the results are discussed.

DIRECT MEASUREMENTS OF THE SIZE AND AMPLITUDE OF IRREGULARITIES IN THE TOPSIDE IONOSPHERE

1. INTRODUCTION

Electron concentration irregularities in the F-region of the ionosphere have been studied using many different observational techniques. In particular much has been learned about the world-wide occurrence characteristics of spread F irregularities from ground-based data (e.g. Reber, 1956; Shimazaki, 1959, 1962; Singleton, 1960, 1968) and more recently from topside sounder data (Calvert and Schmid, 1964; Hice and Frank, 1966; Dyson, 1968). Irregularities in the F-region may be conveniently divided into two classes. The first consists of large scale irregularities known as travelling ionospheric disturbances (Munro, 1950). Because of their large extent, the size and electron concentration variation in these irregularities can be estimated from radio soundings (Munro and Heisler, 1956; Dyson, 1967) or from backscatter observations (Thome, 1964). These irregularities have horizontal dimensions of hundreds of kilometers and electron concentration variations of about 30% (Heisler, 1964) and are the result of internal gravity waves propagating in the neutral atmosphere (Hines, 1960). The second group consists of smaller irregularities which are field-aligned and cause spread F and scintillation of radio signals. The size of these irregularities cannot be determined unambiguously from ionograms. However, sizes in the transverse field direction of between 10 meters and tens of kilometers have been

inferred from observations made using different radio techniques (Herman, 1966a, Bowman, 1960). Variations in electron concentration of between 1% and 70% have been deduced for these irregularities (Herman, 1966a, Singleton, 1962).

Many theories on the production of these irregularities have been suggested and were recently reviewed by Herman (1966a) but none of these can be considered entirely satisfactory at present. Hence there is a definite need for direct measurements of irregularity amplitudes and sizes to check the values inferred from indirect measurements and to determine the extent to which irregularities of different amplitudes and sizes exist simultaneously in the ionosphere. In recent years a number of electrostatic probes have been flown on satellites to measure electron concentration and temperature (e.g., Bowen, et. al., 1964; Brace et. al., 1965; Brace and Reddy, 1965; Sagalyn et. al., 1965). Although these experiments were designed primarily to measure large scale variations in these quantities, small scale electron concentration irregularities are also observed and their size and amplitude can be determined (Brace and Reddy, 1965). This paper presents the results of irregularity observations by the Alouette II electrostatic probe experiment and compares them with the observations made by the topside sounder aboard the same satellite.

2. RESULTS

The Data:

The Alouette II satellite was launched on November 29, 1965 into an elliptical orbit (perigee at 500 km, apogee at 3000 km) with an inclination of 80°. The

topside sounder and electrostatic probe experiments on board this satellite have been described in detail elsewhere (Nelms, et. al. 1966; Franklin and McLean, 1967; Findlay and Brace, 1969) and will not be discussed here. The data used in this study were obtained between August 1 and October 31, 1966 by the tracking stations at Quito, Ecuador; Fort Myers, Florida; Fairbanks, Alaska; and Orroral, Australia. A three month time period was used because it equals half the orbital precession period with respect to the sun and hence is the shortest time over which data at all local times can be obtained. The particular combination of tracking stations employed gives good geomagnetic and geographic latitudinal coverage in both the northern and southern hemispheres and also covers the regions in which topside spread F has previously been studied in detail (Calvert and Schmid, 1954; Hice and Frank, 1966; Dyson 1968).

All the topside ionograms available from these stations during the period specified were examined for the presence of spread F. Topside spread F may be divided into various types (Calvert and Schmid, 1964) but no distinction between these has been made in this study. The electrostatic probe data were also examined for the effects of ionospheric irregularities. The most obvious effects which occur are distortions in individual volt-ampere characteristics, (Figure 1), caused by ionospheric variations along the satellite path. These can result from either electron concentration or temperature variations since the current collected by the probe depends on both of these. However, as shown in Figure 2, electron concentration variations have a much more pronounced

effect and it is unlikely that distortions in individual curves are caused by electron temperature irregularities. (A more detailed discussion is given in the appendix.) The range of irregularity dimensions which can be detected as distortions in individual curves depends on the probe voltage sweep rate and period, the satellite velocity and the response times of the probe electronics and telemetry system. For the Alouette II probe, irregularities up to 3 km in extent along the satellite path can be detected readily. In this analysis "quick look" records of the probe data were used and the lower limit to the size of irregularities which could be resolved (~ 0.2 km) was determined by the film speed used when producing the records rather than by the response times of the electronic systems. The smallest irregularity amplitude which can be detected is a function of its extent along the satellite path (see appendix) and this function for the Alouette II probe is shown in Figure 3. The lower limit of 5% is determined by instrumental effects.

In order to distinguish between the observations of the two experiments, the term "fine structure" will be used to refer to the probe observations of irregularities and the term spread F will be used for the sounder observations. Since the irregularities are probably elongated along the field lines, the spatial extent of the irregularities measured by the probe is related to the transverse dimension of the irregularities. Hence the term "thickness" will be used in discussing the measurements of irregularity size.

Observations of Fine Structure:

Figure 4 shows the percentage occurrence of fine structure as a function of invariant latitude defined by $\cos \Lambda = (1/L)^{1/2}$. This definition orders the data solely in terms of the magnetic field and was used because in the upper F region and the protonosphere electron density irregularities are field-aligned. However since the satellite's perigee is at 500 km, there are no observations at invariant latitudes of less than 15°. The combined effects of the telemetry station locations and the satellite orbital inclination were such that observations were not obtained at latitudes greater than 85° Λ. Figure 4 clearly shows that fine structure occurs almost exclusively in the auroral and polar regions. This result is in agreement with observations made by a similar probe aboard the Explorer 22 satellite (Brace and Reddy, 1965; Dyson and Zmuda, 1968).

The association between the fine structure and the auroral region is further demonstrated in Figure 5 which is a plot of the positions of the auroral oval (Feldstein, 1960) and the equatorward boundary of the fine structure regions. In the case of the latter both northern and southern hemisphere data have been used. The variation in the latitude of the fine structure boundary with local time is similar to that of the auroral oval in that it occurs at lower latitudes at night than during the day. However, the fine structure usually begins as much as 10° equatorward of the oval during night time, and this behavior has also been observed for the irregularities responsible for scintillation (Aarons et. al., 1969). There is a weak tendency for the fine structure boundary to be closer to the

equator during magnetically disturbed conditions. For most passes the data did not extend sufficiently poleward to define a poleward boundary of the fine structure. In the few cases in which a poleward boundary was observed, its location was nearly always poleward of the oval (Figure 5). Thus the fine structure occurs in the same region as the auroral oval but usually extends to both higher and lower latitudes.

For each daytime and nighttime pass in which fine structure occurred the amplitude and thickness of typical irregularities were measured and the results are shown in Figure 6. It should be emphasized that generally irregularities of different sizes are usually observed within each irregularity patch but only the thicknesses and amplitudes typical of each patch have been plotted. The irregularities generally have thicknesses of 0.3 to 1.3 km and amplitudes of about 25%. The daytime irregularities tend to be of smaller amplitude but have thicknesses similar to the nighttime irregularities. No dependence of irregularity size on altitude or Kp was observed.

Observations of Spread F

Since a number of detailed studies on the occurrence characteristics of topside spread F in its various forms have appeared in the literature (e.g. Calvert and Schmid, 1964; Hice and Frank, 1966; Petrie, 1966; Dyson, 1968), we will not discuss these characteristics in detail here. We merely point out that the data used for this study show similar latitudinal and local time variations in

the overall occurrence of spread F (hereafter referred to as spread F_T) to those found in these other studies (see Figure 7). We shall also be concerned with spread F at the satellite height and this will be referred to as spread F_{sat}.

Comparison of Fine Structure and Spread F Observations

The occurrences of spread F_T, spread F_{sat}, and fine structure are compared in Figure 7. The data have been divided into three time periods, nighttime (2000-0400 LT), daytime (0800-1600) and sunrise-sunset (0400-0800 and 1600-2000). Within each time period the data were divided into boxes of 5° invariant latitude and the percentage occurrence calculated for each box. The error bars represent the 90% confidence interval estimate of the population percentage occurrence (Natrella, 1963). Both the northern and southern hemisphere data are included in these figures. Initially individual plots were made for each hemisphere but the difference in the plots was not significant, except for two cases. The two exceptions were the daytime and sunset-sunrise plots of spread F_T which showed greater occurrences at low latitudes in the southern hemisphere than in the northern hemisphere. This difference is also apparent in Hice and Frank's (1966) daytime data. However, combining the data from both hemispheres even in these cases does not affect the conclusions of this study. The sunrise and sunset data were also plotted separately initially and no significant differences were found.

Figure 7 shows that the occurrence of spread F_T at night is very high and there is little change with latitude. In daytime the occurrence at high latitudes is

very high but it decreases rapidly below 60°Λ. At sunset and sunrise an increase with latitude is also apparent but it is not as great as during the day. The occurrence of spread F_{sat} increases with latitude at all times of the day. At high latitudes the occurrence changes little with local time and is almost equal to the occurrence of spread F_T. At mid-latitudes the occurrence of spread F_{sat} is slightly less during the daytime and is always less than the spread F_T occurrence values. The occurrence of fine structure also increases with latitude and there is a large diurnal variation, with the maximum occurrence at night. During the night, the occurrence of fine structure is much less than that of spread F_{sat} except at high latitudes where the occurrences are approximately the same. Examination of ionograms and probe records obtained simultaneously showed that whenever fine structure was present spread F_{sat} occurred. Furthermore the degree of spreading was generally greater when fine structure was observed (Table 1). This result is consistent with Petrie's (1966) observation that the maximum amount of spread F_{sat} occurs in the auroral oval region.

3. INTERPRETATION OF RESULTS

The results presented in the last section show that the occurrence of spread F_{sat} is significantly less than that of spread F_T, particularly at mid latitudes. This suggests that the irregularities causing spread F often exist below the satellite but do not extend up to it. However, there are qualifying factors which must be considered. Firstly, when the satellite is near apogee (3000 km), the electron scale height is very great. As a result the virtual height changes very

rapidly with frequency so that echoes from near the satellite height are very weak and do not appear on the ionograms. Hence it is difficult to determine if spread F_{sat} is present in these cases. Secondly when combination mode spread F (Muldrew, 1963) occurs, extra echoes may not be observed at the satellite height even though irregularities responsible for these echoes probably extend up to the satellite. The differences between the occurrences of spread F_T and spread F_{sat} are probably due largely to these limitations rather than any variation in occurrence with altitude and hence the occurrence of spread F_{sat} represents a lower limit to the actual occurrence of irregularities at the satellite height.

The fine structure observations indicate the presence of irregularities in the immediate vicinity of the satellite. Therefore we might expect some similarity between the occurrences of fine structure and spread F_{sat}. The results show (Figure 7) that even though the occurrence of spread F_{sat} represents a lower limit for the occurrence of irregularities at this height, the occurrence of fine structure is generally even smaller. Therefore irregularities are often present at the satellite height which can cause spread F but are not detectable as probe fine structure. Figure 7 shows that this occurs more often at mid-latitudes indicating that irregularities of different sizes occur at different latitudes. Since spread F_{sat} is observed whenever fine structure is, it is relevant to examine whether the irregularities causing the fine structure are the same ones responsible for the spread F.

In the topside ionosphere irregularities are field aligned and extend for large distances along field lines since diffusion in the direction of the magnetic field is the dominating process. Thus we can approximate irregularities in the vicinity of the satellite to thin field-aligned layers (Figure 8). Consider the case in which the layers are parabolic. If we ignore the effect of the magnetic field, the refractive index, n, at a frequency f, is given by

$$n^2(z) = 1 - \frac{f_c^2}{f^2} - \frac{f_b^2 - f_c^2}{f^2} \left(\frac{2z}{t}\right)^2$$

where

t is the thickness of the layer

f_c is the critical frequency of the layer

z is a distance parameter

f_b is the plasma frequency of the background medium

Following the method used by Rydbeck (1942), the reflection coefficient for such a layer is given by

$$R^2 = (1 + e^{-2\pi\rho})^{-1}$$

where

$$\rho = \frac{\pi t}{2c} \frac{f_c^2 - f^2}{\sqrt{f_c^2 - f_b^2}}$$

c is the velocity of light. The sensitivity of the Alouette II sounder receiver is about 116 d.b. (Franklin and McLean, 1967) so that, for an irregularity with

amplitude 100 x %, the thickness of an irregularity causing a frequency spread Δf is given by

$$t = \frac{26.71\ c\ x^{1/2}\ X_b}{\pi^2\ f_b\ [1 - (1 + x)\ X_b]}$$

where

$$X_b = (f_b/(f_b + \Delta f))^2$$

Figure 9 shows plots of t as a function of x for various values of f_b and Δf. When fine structure was observed f_b was typically less than 1 MHz and $\Delta f \geq 1$ MHz. Hence the irregularities responsible were less than 0.4 km thick and correspond to the thinnest irregularities observed to cause fine structure (Figure 6). When spread F_{sat} is observed but fine structure is not, the frequency spreading is usually less than 1 MHz (see table 1). The echo configurations which normally occur on topside ionograms when spread F_{sat} is present indicate that thin field-aligned irregularities are responsible (Calvert and Schmid, 1964). Figure 9 shows that when the plasma frequency is less than 2 MHz, irregularities less than 0.5 km thick and with amplitudes less than 5% could cause spread F but not resolvable fine structure. This value for the thickness of the irregularities agrees with the results of most other techniques which indicate thickness of about 1 km or less (see Herman, 1966a). An exception concerns Bowman's observations of bottomside spread F which he interpreted as being caused by wave like irregularities with horizontal wavelengths of tens of kilometers (Bowman, 1960). Such waves would most likely result from gravity

waves in the neutral atmosphere, however, since the amplitude of gravity waves is heavily attenuated in the upper atmosphere they could not be responsible for irregularities in the upper F region and protonosphere.

4. DISCUSSION

It has long been recognied (Shimazaki, 1959; Singleton, 1960; Piddington, 1964) that different irregularity production mechanisms are very likely operative at different latitudes. This is supported by our results which show that irregularities in the region of the auroral oval often are of a different size and amplitude to those at mid-latitudes.

One possible source of the oval irregularities is the precipitating particles that occur in this region. Herman (1966b) has shown that proton fluxes can produce sufficient ionization to cause such irregularities. Because the protons precipitate along field lines and are not scattered appreciably by the collisions they undergo, each proton produces ionization that is field aligned and contained within a tube of radius equal to the gyro-radius of the proton. To produce electron density irregularities would require spatial variations in the intensity of the precipitating proton flux, however, no rapid spatial variations have been observed (Eather, 1967). Although precipitating electrons are scattered more by collisions they will remain within a field aligned tube of radius several times the gyroradius at least in the region above 90 km where they produce most of their ionization (Chamberlain, 1961). Therefore precipitating electrons could

also produce irregularities in electron density. Particle detectors aboard satellites have observed large changes in electron flux over distances of about a kilometer but it is possible that these variations are temporal rather than spatial, (Evans et. al., 1967). In fact intense fluxes of low energy electrons ($E \geq 10$ kev) are observed at invariant latitudes as low as 60° (Fritz and Gurnett, 1965) so that if the irregularities are related to electron precipitation it is not surprising that they occur over a region more extensive than the auroral oval. Probably then, precipitating electrons are more likely to be the cause of irregularities than are protons. Since spatial variations in the precipitating flux intensity are required in this mechanism the ultimate cause of the irregularities would be related to the magnetospheric processes.

Another mechanism which produces irregularities in the auroral region is that proposed by Piddington (1964). In this mechanism frictional forces in the magnetosphere cause a Pedersen drift in the E region resulting in irregularities with horizontal dimensions the order of 1 km. The irregularities are transferred to the F region by polarization fields. The mechanism is restricted to the auroral region because the Pedersen drift is zero elsewhere. A test of this theory would be to determine if the F region irregularities extend down into the E-region but this cannot be done using satellite observations alone. Dessler (1958) postulated that F region irregularities were caused by hydromagnetic waves and Singleton (1962) showed that this mechanism would produce irregularities with the largest amplitudes in the auroral region. This is consistent with

the observations reported here but this theory gives no explicit way of calculating irregularity dimensions to compare with those observed. With these limitations it is not possible to decide between these mechanisms using the data reported here. It is possible that all these mechanisms occur and they may in fact be related to one another. For example, the magnetospheric forces responsible for the Pedersen drift in the E region may also affect the intensity of the precipitation flux along the same field lines.

At midlatitudes the irregularities cannot be produced directly by precipitating particles or Pedersen drift, although it is possible that the irregularities produced in the auroral zone drift to lower latitudes under the influence of the Sq and DS electric fields (Piddington, 1964). As the irregularities drift equatorward they will decrease in amplitude and increase in thickness due to diffusion processes. Thus this mechanism produces irregularities at mid latitudes which have different characteristics to those in the auroral zone, a feature that is supported by the electrostatic probe observations. The hydromagnetic wave mechanism is still operative at mid-latitudes and produces smaller amplitude irregularities than in the auroral zone (Singleton, 1962).

Another possible mechanism at mid-latitude is that proposed by Bowhill (1966) in which irregularities result from changes in the heat flux conducted from the protonosphere to the ionosphere. His calculations showed that a change in the nighttime heat flux from 10^8 to 3×10^8 eV cm^{-2} sec^{-1} would

cause a decrease in the electron density of about 10% at the F_2 peak and an increase of 30% or more at 1000 km. However, our results indicate that mid-latitude irregularities above 1000 km have amplitudes more like 5% so that smaller changes in the heat flux would be sufficient. In fact irregularities with amplitudes of a few percent could be produced in the topside ionosphere by changes in the heat flux even in the daytime and this may explain why daytime mid-latitude spread F occurs more often in the topside ionosphere than the bottomside ionosphere (Dyson, 1968).

5. SUMMARY

In the topside ionosphere, electron density irregularities, observed by the Langmuir probe occur in patches several hundred kilometers in extent and have thicknesses less than 2 km and amplitudes between 5% and 70%. They occur in a region which encompasses the auroral oval and extends further poleward and equatorward of the oval. Spread F observed simultaneously by the Alouette II sounder was caused by the irregularities less than 0.4 km thick. At mid-latitudes irregularities are also observed, but these are probably larger and have amplitudes of less than 5%. There are several theories on the production of irregularities which would account for the observations. Further measurements of irregularity thicknesses and amplitudes would enable these theories to be examined more critically. Although a large amount of electrostatic probe data from satellites is available, the information it contains on small scale irregularities is limited because the experiments design was not optimum for irregularity

measurements. It would be extremely valuable to employ a modified experimental arrangement whereby irregularities with amplitudes of 1% or less and with dimensions of as much as tens of kilometers could be measured. Such an experiment (to be flown on a future sounder satellite) could readily resolve the question of whether in the region of the F_2 peak, spread F is caused by irregularities of about 1 km thick (Herman, 1966a) or by wave-like irregularities with wavelengths of the order of 10 km (Bowman, 1960, 1968).

ACKNOWLEDGEMENTS

I would like to thank the National Academy of Sciences for a NAS-NASA Resident Research Associateship and L. H. Brace for helpful discussions and for making the Langmuir probe data available. The Alouette II ionograms were kindly supplied by the Data Center at Goddard Space Flight Center.

APPENDIX

EFFECT OF IRREGULARITIES ON ELECTROSTATIC PROBE AMPERE-VOLT CHARACTERISTICS

The electron current to a stationary cylindrical probe is given by (Mott-Smith and Langmuir, 1926)

$$I_e = AN_e e\sqrt{\frac{kT_e}{2\pi m}}\left\{2\sqrt{\frac{\eta}{\pi}} + \exp(\eta)\ \left[1 - \operatorname{erf}\sqrt{\eta}\right]\right\} \quad \eta > 0 \tag{1}$$

$$= AN_e e\sqrt{\frac{kT_e}{2\pi m}}\exp(\eta) \quad \eta < 0 \tag{2}$$

where

$\eta = eV/kT_e$

A = is the area of the probe

N_e = is the electron density

m = is the electron mass

e = is the electronic charge

T_e = is the electron temperature

k = is Boltzmann's constant

V = is the applied voltage.

Similar equations apply for the ion current and a theoretical probe characteristic is shown in Figure 10.

Using these equations and assuming the shape and size of electron density or electron temperature irregularities we can readily calculate the ampere-volt (I-V) characteristics which would result if a satellite-borne probe passed through such irregularities. Examples of theoretical I-V characteristics for different types of irregularities are shown in Figure 2.

Theoretically it would be possible to detect ionospheric irregularities by determining whether or not the I-V curves deviate from the shape obtained when the medium is homogeneous. However, this approach would be difficult because corrections would have to be made for probe orientation affects. A simpler approach is to consider only those irregularities which produce sufficiently large distortions in individual probe characteristics so that they are readily detected by visually scanning the data records (i.e., distortions similar to those of Figure 1). The arbitrary criterion has been adopted that only irregularities large enough to cause $d I_e / d\eta \leq 0$ have been considered.

Because the satellite is moving the quantity that determines whether or not $d I_e / d\eta$ becomes less than or equal to zero is the N_e or T_e gradient along the satellite path. Differentiating equations (1) and (2) with respect to x, the distance along the satellite path, we have for the electron saturation region.

$$\frac{1}{I_e}\frac{dI_e}{dx} = \frac{1}{N_e}\frac{dN_e}{dx} + \frac{1}{T_e}\frac{dT_e}{dx}\left\{0.5 - \frac{\eta}{1 + 2\sqrt{\eta}/\sqrt{\pi}\, e^{\eta}\,(1 - \operatorname{erf}\sqrt{\eta})}\right\} + \frac{e}{kT_e}\left\{\frac{1}{1 + 2\sqrt{\eta}/\sqrt{\pi}\, e^{\eta}\,(1 - \operatorname{erf}\sqrt{\eta})}\right\}\frac{dV}{dx} \qquad (1A)$$

and for the electron retardation region

$$\frac{1}{I_e}\frac{dI_e}{dx} = \frac{1}{N_e}\frac{dN_e}{dx} + \frac{1}{T_e}\frac{dT_e}{dx}(0.5 - \eta) + \frac{e}{kT_e}\frac{dV}{dx} \qquad (2A)$$

$$\frac{dV}{dx} = \frac{R}{v}$$

where R is the voltage sweep rate and v is the satellite velocity. In deriving these equations changes in the satellite potential due to changes in T_e have been ignored.

If we consider first the electron saturation region then the requirement $dI_e/d\eta \leq 0$ means that electron density irregularities will be detected if

$$-\frac{1}{N_e}\frac{dN_e}{dx} \geq \frac{e}{kT_e}\left\{\frac{1}{1 + 2\sqrt{\eta}/\sqrt{\pi}\, e^{\eta}(1 - \mathrm{erf}\sqrt{\eta})}\right\}\frac{dV}{dx} \qquad (1B)$$

and T_e irregularities will be detected if

$$-\frac{1}{T_e}\frac{dT_e}{dx} \geq \frac{e}{kT_e}\left\{\frac{1}{1 + 2\sqrt{\eta}/\sqrt{\pi}\, e^{\eta}(1 - \mathrm{erf}\sqrt{\eta})}\right\}\frac{dV}{dx}\Bigg/\left\{0.5 - \frac{\eta}{1 + 2\sqrt{\eta}/\sqrt{\pi}\, e^{\eta}(1 - \mathrm{erf}\sqrt{\eta})}\right\}$$

(2C)

In the electron retardation region the requirement for N_e irregularities to be detected is that

$$-\frac{1}{N_e}\frac{dN_e}{dx} \geq \frac{e}{kT_e}\frac{dV}{dx} \qquad (2B)$$

and for T_e irregularities

$$-\frac{1}{T_e}\frac{dT_e}{dx} \geq \frac{e}{kT_e}\frac{dV}{dx}\Big/\{0.5 - \eta\}. \qquad (2C)$$

In Figure 11 the values of $(1/N_e)(dN_e/dx)$ and $(1/T_e)(dT_e/dx)$ for which $dI/d\eta = 0$ have been plotted as a function of applied voltage for the Alouette II probe. Above zero volts (the plasma potential) the effect of N_e irregularities on the probe characteristics is much greater than T_e irregularities. At negative voltages T_e irregularities affect the curves more but even at -2V very large gradients in T_e would be required to cause an inflection point in the I-V curve. At more negative voltages the main component of the probe current is that due to positive ions and any distortions occurring in the I-V curves would more likely be caused by density irregularities than temperature variations.

Under typical conditions, the Alouette II probe sweeps to at least 8 volts above the plasma potential. Thus from Figure 11 it is apparent that irregularities must have gradients of about 0.2/km or more to be detected, i.e., an irregularity 1 km thick must have an amplitude of at least 10%.

Table 1

	Fine Structure	
Spread F_{sat}	Yes	No
< 1 MHz	58	230
≥ 1 MHz	113	21

Number of observations of fine structure and spread F_{sat} .

REFERENCES

Aarons, J., J. P. Mullen, and H. E. Whitney, The Scintillation boundary, J. Geophys. Res., 74, 884, 1969.

Bowen, P. J., R. L. F. Boyd, C. L. Henderson, A. P. Willmore, Measurement of electron temperature and concentration from a spacecraft, Proc. Roy. Soc. A, 281, 514, 1964.

Bowhill, S. A., Origin of field-aligned irregularities in the F_2 layer, Spread F and its effects upon radiowave propagation and Communication, Technivision, England, 1966.

Bowman, G. G., Further studies of 'spread-F' at Brisbane, 2, Interpretation, Planetary Space Sci., 2, 150, 1960.

Bowman, G. G., The nature of spread-F irregularities in Antarctica, Aust. J. Phys., 21, 695, 1968.

Brace, L. H., and B. M. Reddy, Latitudinal variations of electron temperature and concentration from satellite probes, NASA X-651-65-190, 1965.

Brace, L. H., N. W. Spencer, and A. Dalgarno, Detailed behaviour of the mid-latitude F region from Explorer 17 satellite, Planetary Space Sci., 13, 647, 1965.

Calvert, W., and C. W. Schmid, Spread F observations by the Alouette topside sounder satellite, J. Geophys. Res., 69, 1839, 1964.

Chamberlain, J. W., Physics of the Aurora and Airglow, Academic Press, New York, 1961.

Dessler, A. J., Large amplitude hydromagnetic waves above the ionosphere, J. Geophys. Res., 63, 507, 1958.

Dyson, P. L., Topside refractive irregularities and travelling ionospheric disturbances, Aust. J. Phys., 20, 467, 1967.

Dyson, P. L., Topside spread F at midlatitudes, J. Geophys. Res., 73, 2441, 1968.

Dyson, P. L., and A. J. Zmuda, Electrostatic Probe Observations of the ionosphere at 1000 kilometers altitude within the auroral oval, NASA X-621-68-409, 1968.

Eather, R. H., Auroral proton precipitation and hydrogen emissions, Rev. Geophys., 5, 207, 1967.

Evans, J. S., R. G. Johnson, R. D. Sharp, and J. B. Reagan, Recent results from satellite measurements of low-energy particles precipitated at high latitudes, Space Sci. Rev. 7, 263, 1967.

Feldstein, Y. I., Some problems concerning the morphology of auroras and magnetic disturbances at high latitudes, Geo. and Aer. 3, 183, 1963.

Findlay, J. A. and L. H. Brace, Cylindrical Electrostatic Probes Employed on Alouette II and Explorer 31 Satellites, to be published in Proc. I.E.E.E., 1969.

Franklin, C. A., and M. A. MacLean, The Alouette II Topside Ionospheric Sounder, presented at the International Conference on Electronics and Space, Paris, 1967.

Fritz, T. A., and D. A. Gurnett, Diurnal and latitudinal effects observed for 10-kev electrons, J. Geophys. Res., 70, 2455, 1965.

Heisler, L. H., Major F region irregularities, Radio Res. Board Symp. on Ionospheric Irregularities, 25, 1964.

Herman, J. R., Spread F and ionospheric F region irregularities, Rev. Geophys., 4, 255, 1966a.

Herman, J. R., A charged particle production mechanism for spread-F irregularities, Spread F and its effects upon radiowave propagation and communication, Technivision, England, 1966b.

Hice, J. D., and B. Frank, Occurrence patterns of topside spread F on Alouette ionograms, J. Geophys. Res., 71, 3653, 1966.

Hines, C. O., Internal atmospheric gravity waves at ionospheric heights, Canadian J. Phys., 38, 1441, 1960.

Mott-Smith, H. M., and I. Langmuir, The theory of collectors in gaseous discharges, Phys. Rev., 28, 727, 1926.

Muldrew, D. B., Radio propagation along magnetic field-aligned sheets of ionization observed by the Alouette topside sounder, J. Geophys. Res., 68, 5355, 1963.

Munro, G. H., Travelling disturbances in the ionosphere, Proc. Roy. Soc. A, 219, 447, 1953.

Munro, G. H., and L. H. Heisler, Cusp Type Anomalies in Variable Frequency Ionospheric Records, Aust. J. Phys., 9, 343, 1956.

Natrella, Mary G., Experimental Statistics, N. B. S. Handbook 91, U. S. Government Printing Office, Washington, 1963.

Nelms, G. L., R. E. Barrington, J. S. Belrose, T. R. Hartz, I. B. McDiarmid, and L. H. Brace, The Alouette II Satellite, Canadian J. Phys., 44, 1419, 1966.

Petrie, L. E., Preliminary results on mid and high latitude topside spread F, Spread F and its effects upon radiowave propagation and communication, Technivision, England, 1966.

Piddington, J. H., Irregularities in the upper ionosphere, Planetary Space Sci., 12, 127, 1964.

Reber, G., Worldwide spread F, J. Geophys. Res., 61, 157, 1956.

Rydbeck, O. E. H., The reflection of electromagnetic waves from a parabolic friction-free ionized layer, J. Applied Phys., 13, 577, 1942.

Sagalyn, R. C., M. Smiddy, and Y. N. Bhargava, Satellite measurements of the diurnal variation of electron temperatures in the F region, Space Research, V, 189, 1965.

Shumazaki, T., A statistical study of world-wide occurrence probability of spread F, 1, Average state, J. Radio Res. Lab., Japan, 6, 669, 1959.

Shumazaki, T., A statistical study of occurrence probability of spread F at high latitudes, J. Geophys. Res., 67, 4617, 1962.

Singleton, D. G., The Geomorphology of spread F, J. Geophys. Res., 65, 3615, 1960.

Singleton, D. G., Spread-F and the parameters of the F-layers of the ionosphere, 4, Causative mechanisms, J. Atmospheric Terrest. Phys., 24, 909, 1962.

Singleton, D. G., The morphology of spread-F occurrence over half a sunspot cycle, J. Geophys. Res., 73, 295, 1968.

Thome, G. D., Incoherent scatter observations of travelling ionospheric disturbances, J. Geophys. Res., 69, 4047, 1964.

FIGURE CAPTIONS

Figure 1. Volt-ampere characteristics obtained from the Alouette II probe (a) normal record, (b) curves distorted due to ionospheric irregularities. For details concerning the data see Findlay and Brace (1969).

Figure 2. Theoretical volt-ampere characteristics when irregularities present (a) Gaussian electron density irregularities of 30% amplitude (b) Gaussian electron temperature irregularities of 30% amplitude.

Figure 3. Minimum amplitude of electron density irregularities which can be detected by the Alouette II probe. The lower limit of resolution (5%) is due to instrumental effects.

Figure 4. The percentage occurrence of fine structure plotted against invariant latitude Λ ($\cos^2 \Lambda = 1/L$).

Figure 5. Locations of the equatorward and poleward boundaries of fine structure and the auroral oval (after Feldstein, 1963).

Figure 6. Histograms showing typical amplitudes and thicknesses of the irregularities causing fine structure during daytime (0800-1600 LMT) and nighttime (2000-0400 LMT).

Figure 7. The occurrence of spread F_T (overall spread F), spread F_{sat} (spread F at the satellite height), and fine structure at (a) nighttime, (b) day time, (c) sunset-sunrise.

Figure 8. Model of electron density irregularities used to estimate thickness of irregularities causing spread F_{sat}.

Figure 9. Plots of irregularity thickness as a function of irregularity amplitude for various values of the plasma frequency, f_b, and the amount of frequency spreading, Δf. Irregularities in the shaded zone cannot be detected by the probe.

Figure 10. Theoretical volt-ampere characteristic.

Figure 11a. Minimum electron density gradients required to produce detectable fine structure. N_e gradients are detected more readily in the electron saturation region of the ampere-volt characteristic.

Figure 11b. Minimum electron temperature gradients required to produce detectable fine structure. T_e gradients have the greatest effect in the retardation region of the ampere-volt curve.

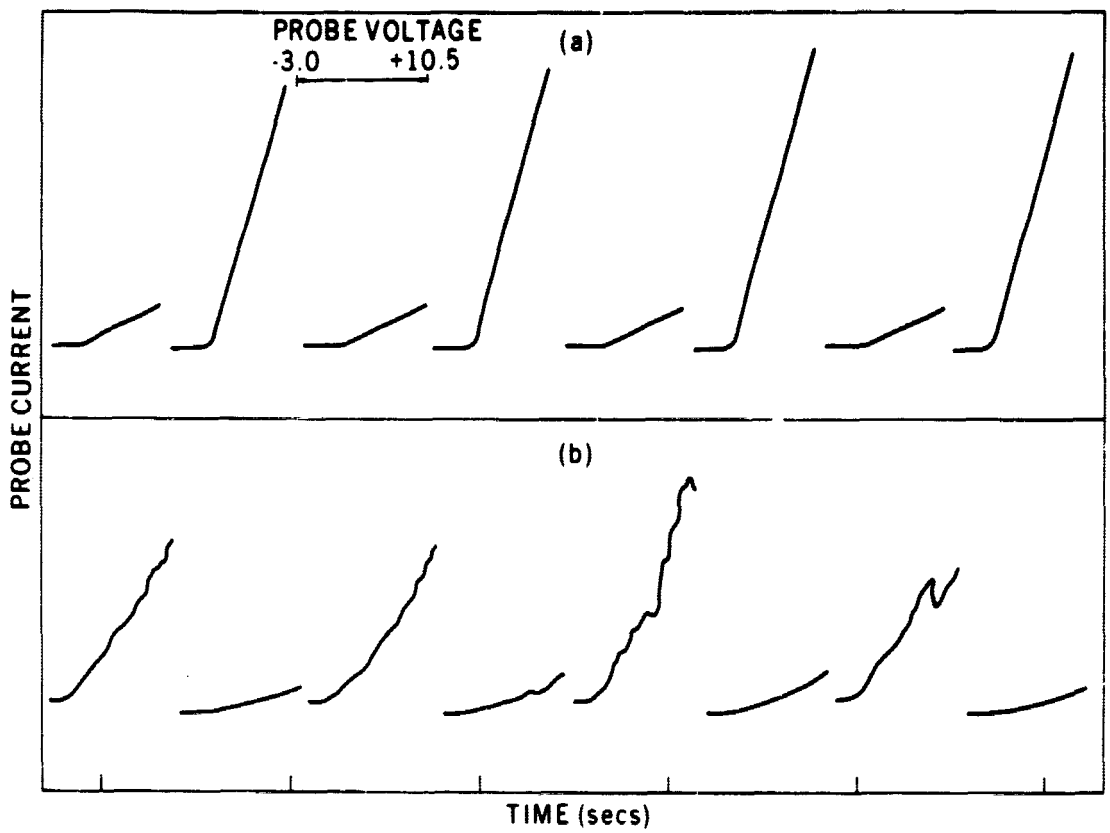

Figure 1–Volt-ampere characteristics obtained from the Alouette II probe (a) normal record, (b) curves distorted due to ionospheric irregularities. For details concerning the data see Findlay and Brace (1969).

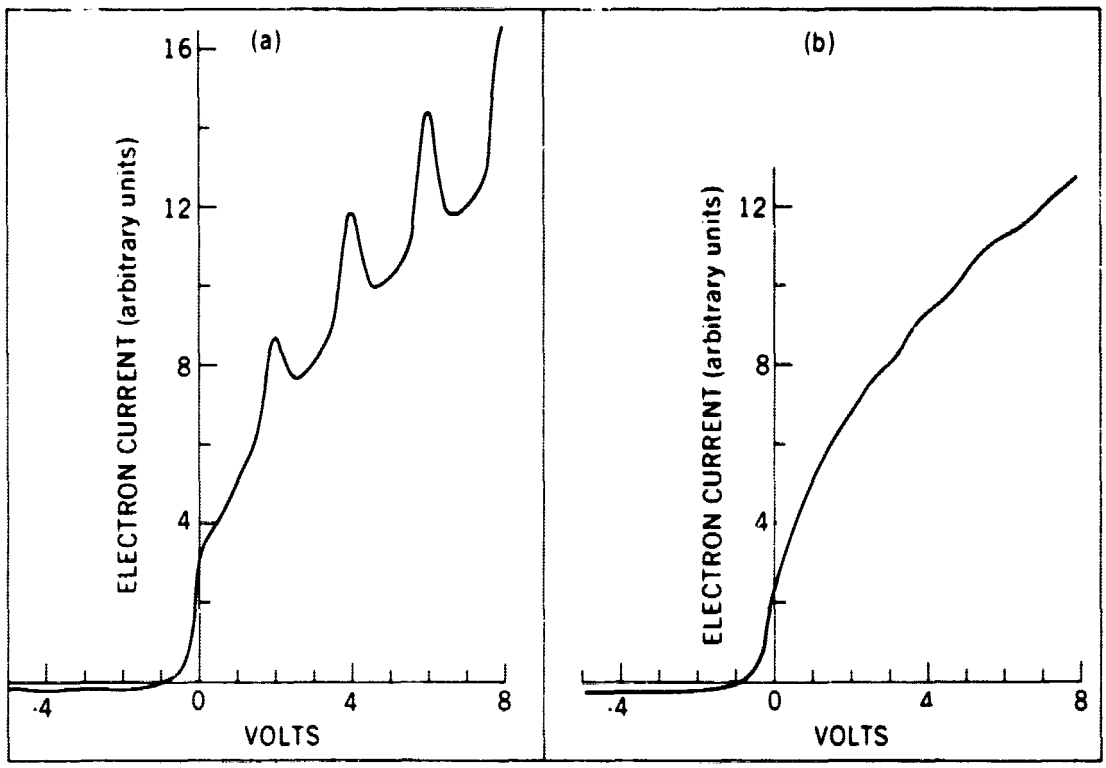

Figure 2–Theoretical volt-ampere characteristics when irregularities present (a) Gaussian electron density irregularities of 30% amplitude (b) Gaussian electron temperature irregularities of 30% amplitude.

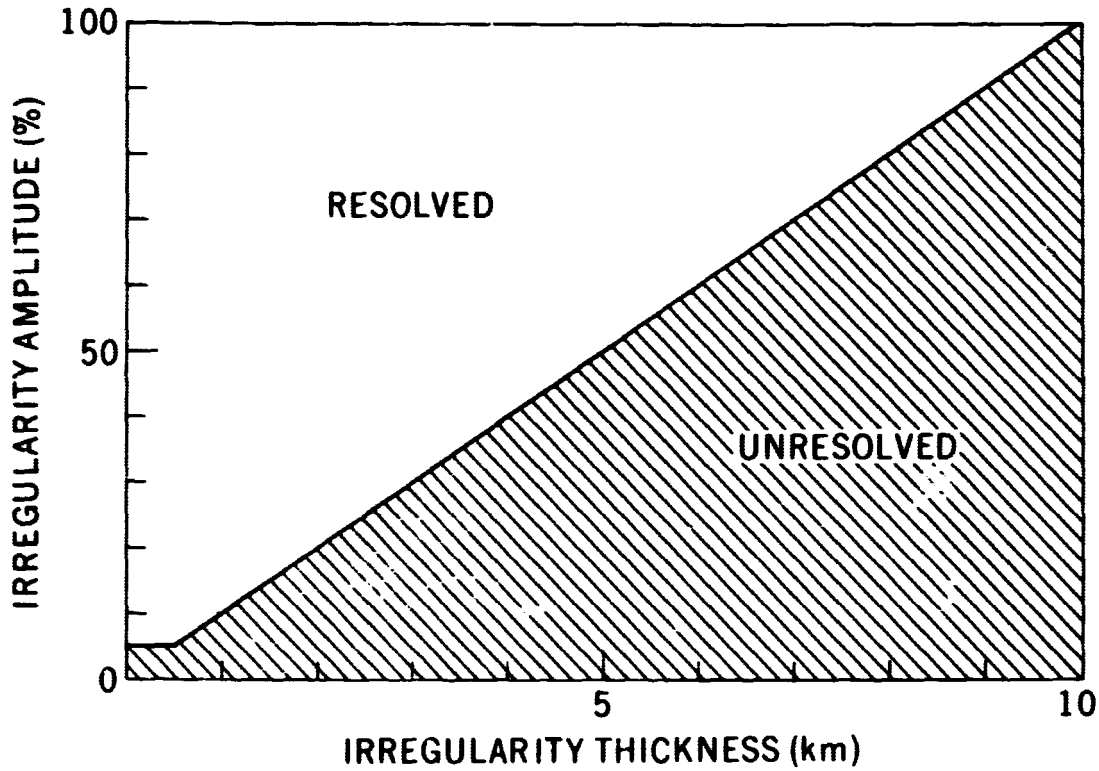

Figure 3–Minimum amplitude of electron density irregularities which can be detected by the Alouette II probe. The lower limit of resolution (5%) is due to instrumental effects.

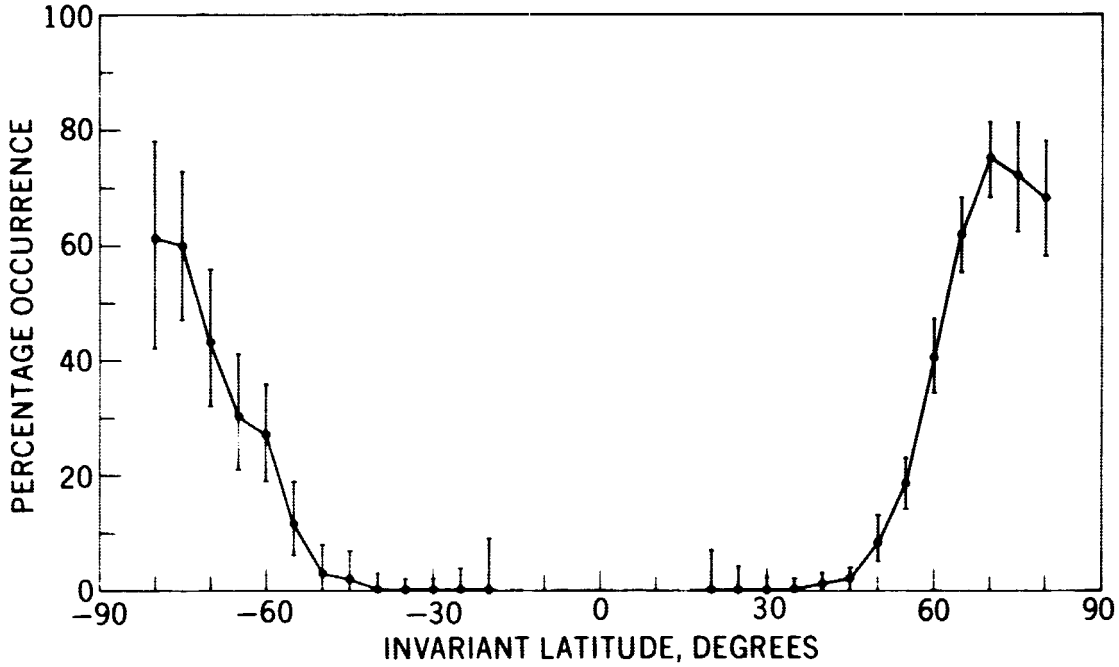

Figure 4–The percentage occurrence of fine structure plotted against invariant latitude Λ ($\cos^2 \Lambda = 1/L$).

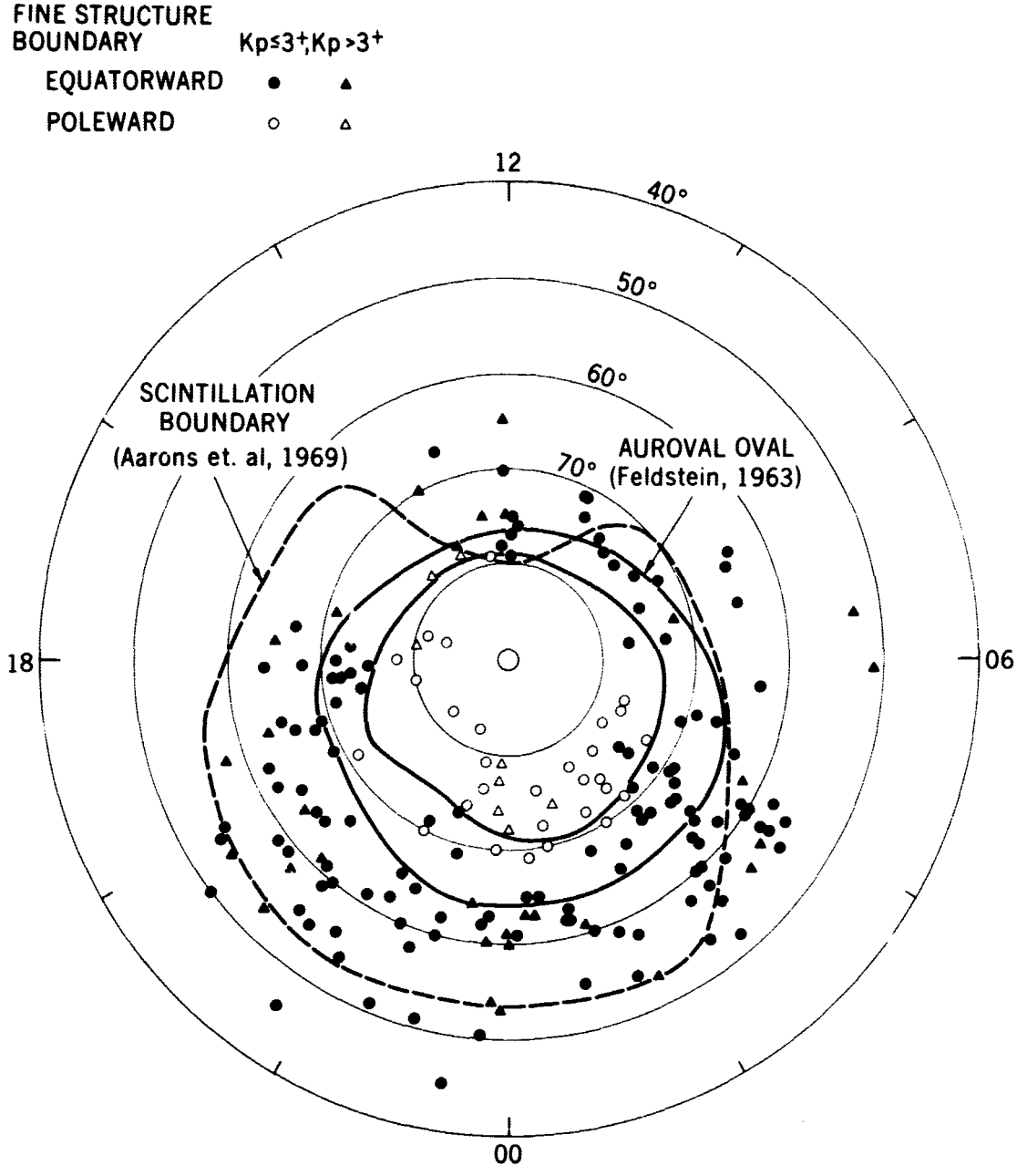

Figure 5–Locations of the equatorward and poleward boundaries of fine structure and the auroral oval (after Feldstein, 1963).

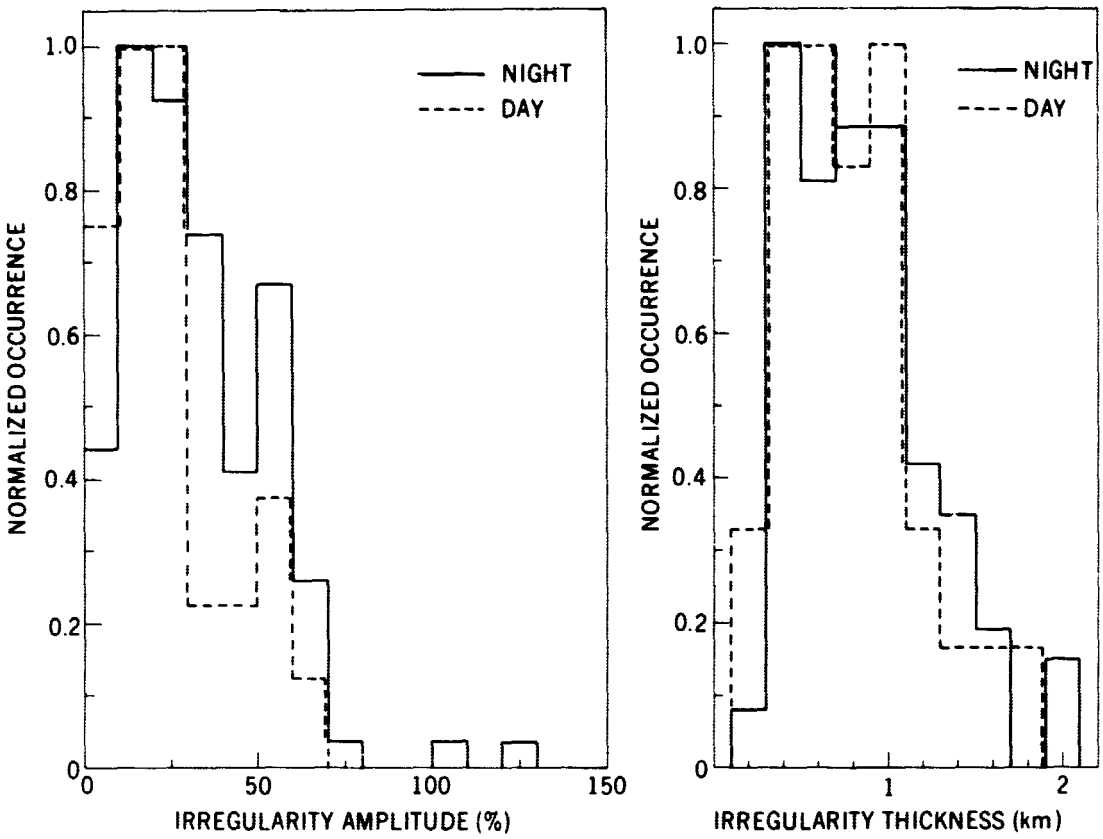

Figure 6–Histograms showing typical amplitudes and thicknesses of the irregularities causing fine structure during daytime (0800–1600 LMT) and nighttime (2000–0400 LMT).

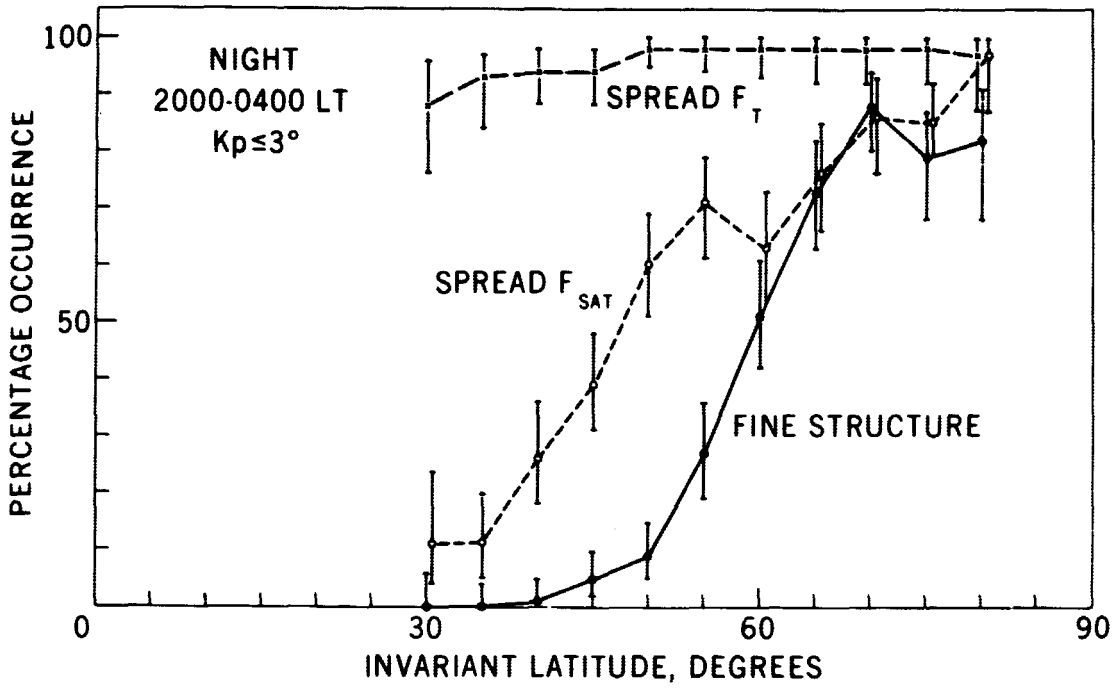

Figure 7a—The occurrence of spread F_T, spread F_{sat}, and fine structure at nighttime

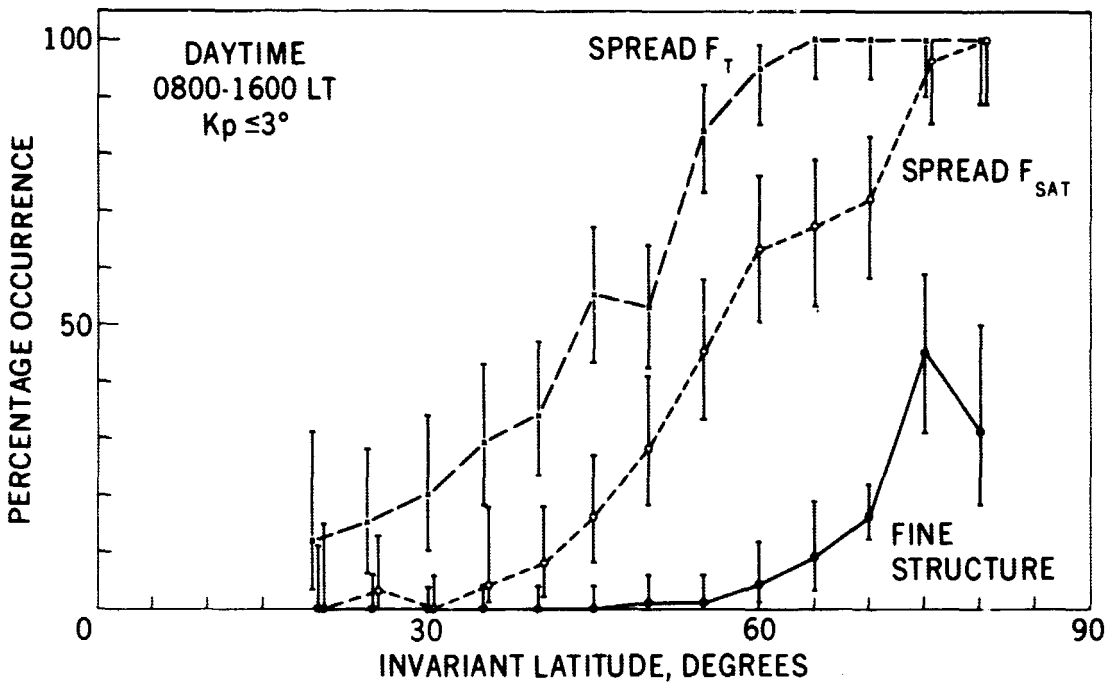

Figure 7b–The occurrence of spread F_T (overall spread F), spread F_{sat} (spread F at the satellite height), and fine structure during daytime.

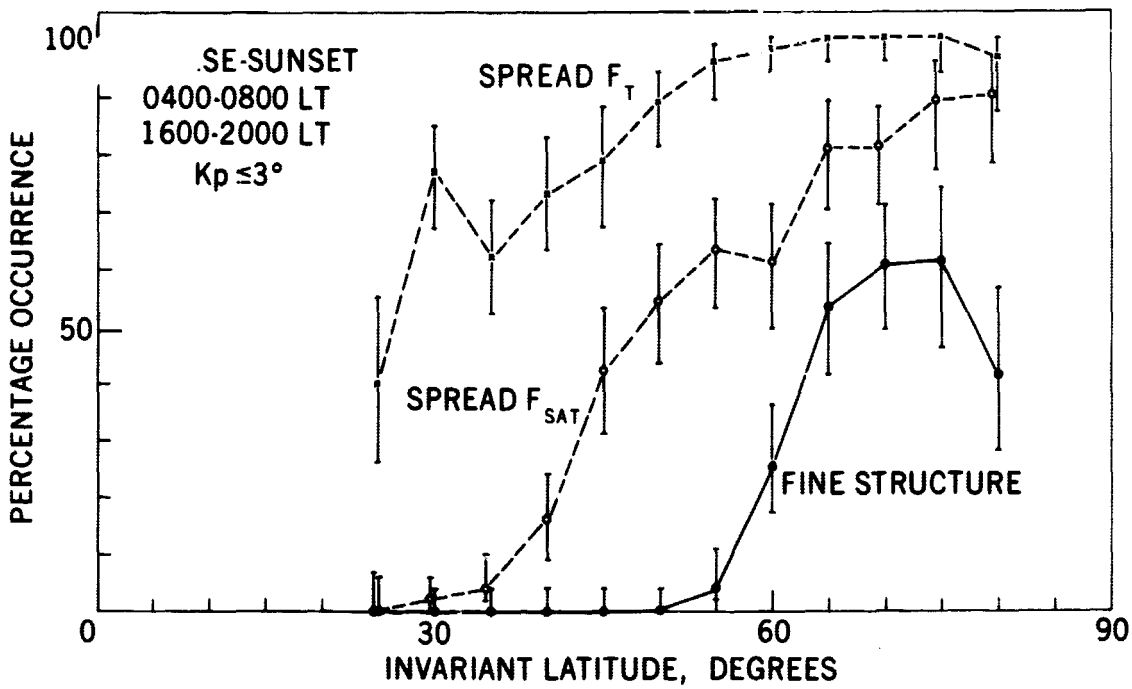

Figure 7c—The occurrence of spread F_T, spread F_{sat}, and fine structure at sunrise-sunset

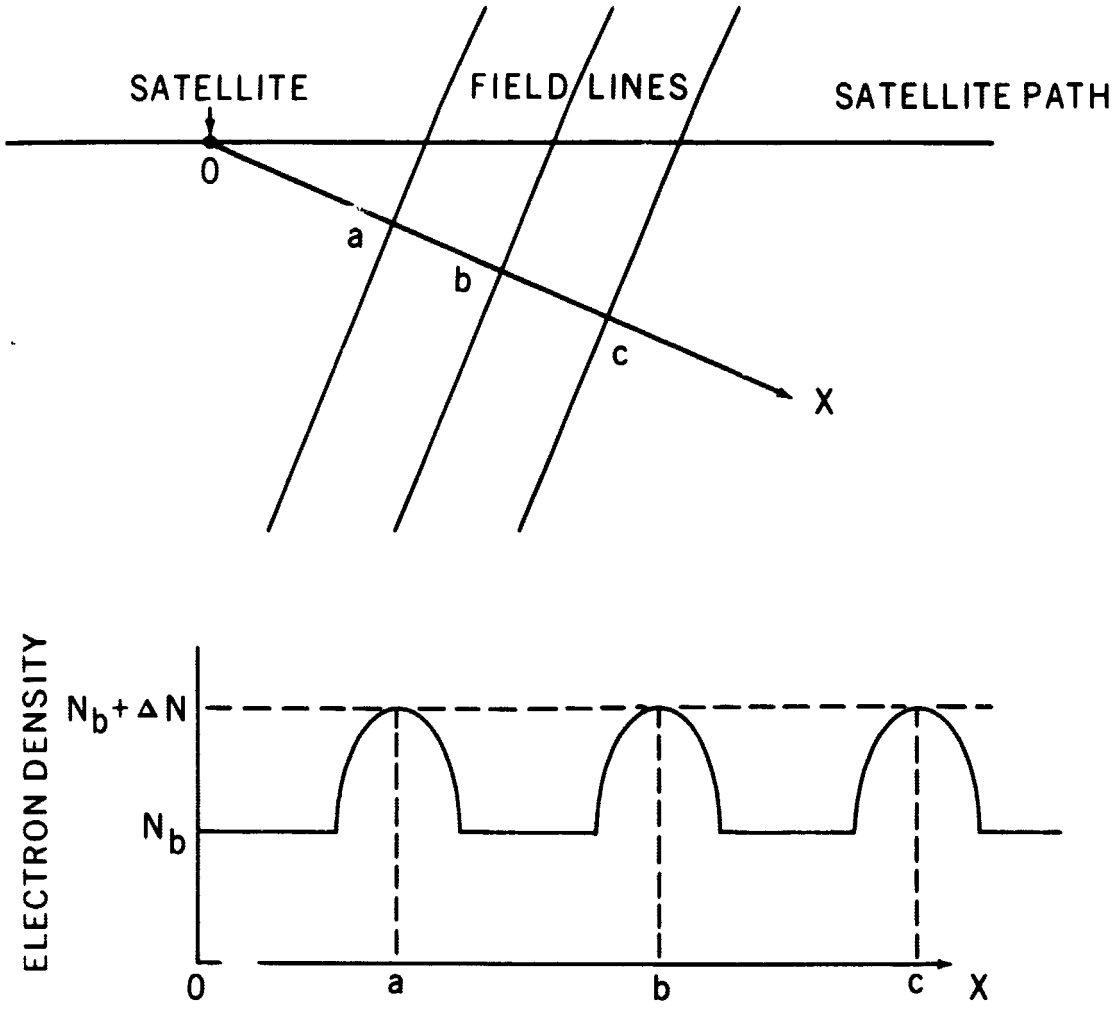

Figure 8–Model of electron density irregularities used to estimate thickness of irregularities causing spread F_{sat}.

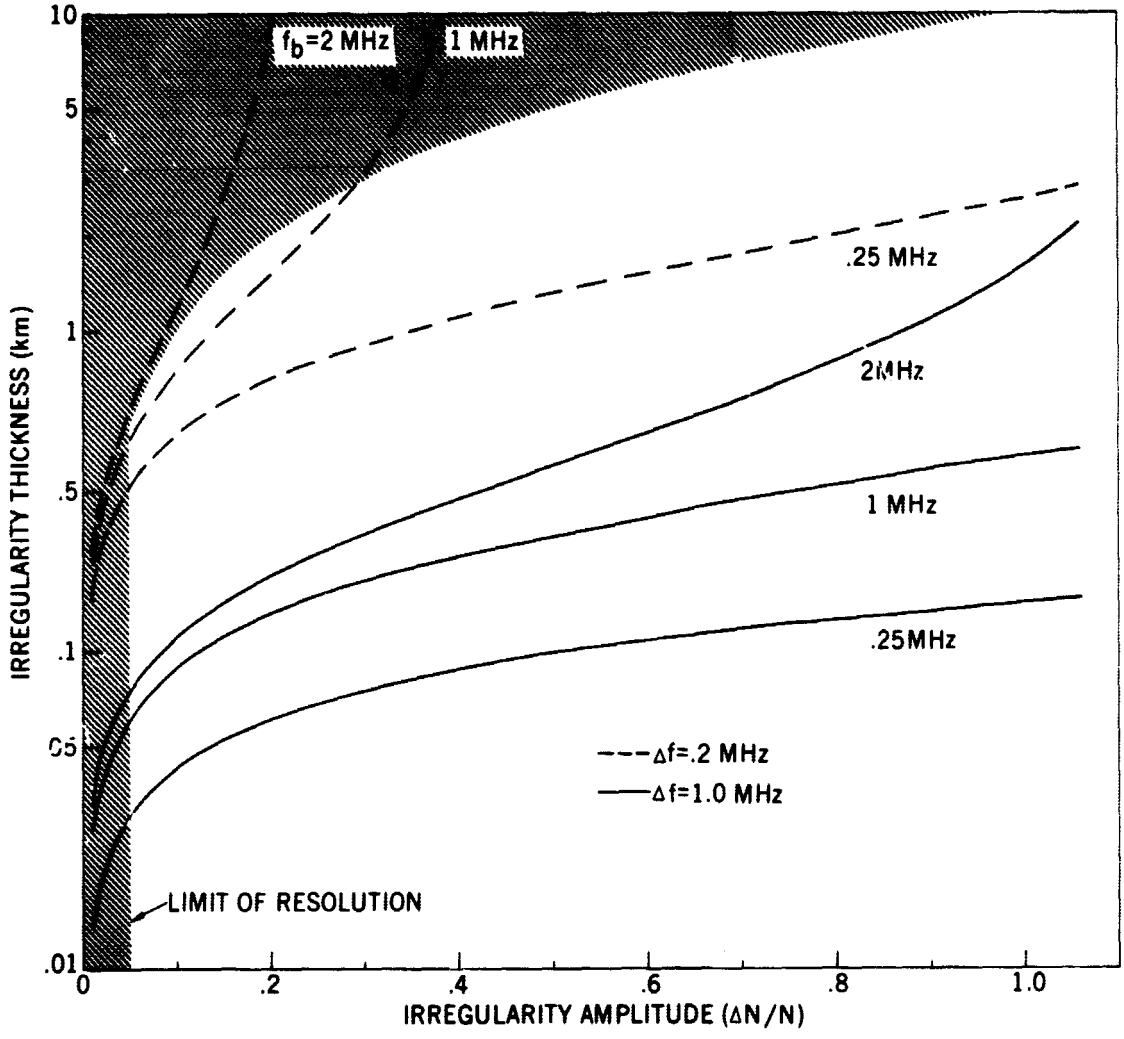

Figure 9–Plots of irregularity thickness as a function of irregularity amplitude for various values of the plasma frequency, f_b, and the amount of frequency spreading, Δf. Irregularities in the shaded zone cannot be detected by the probe.

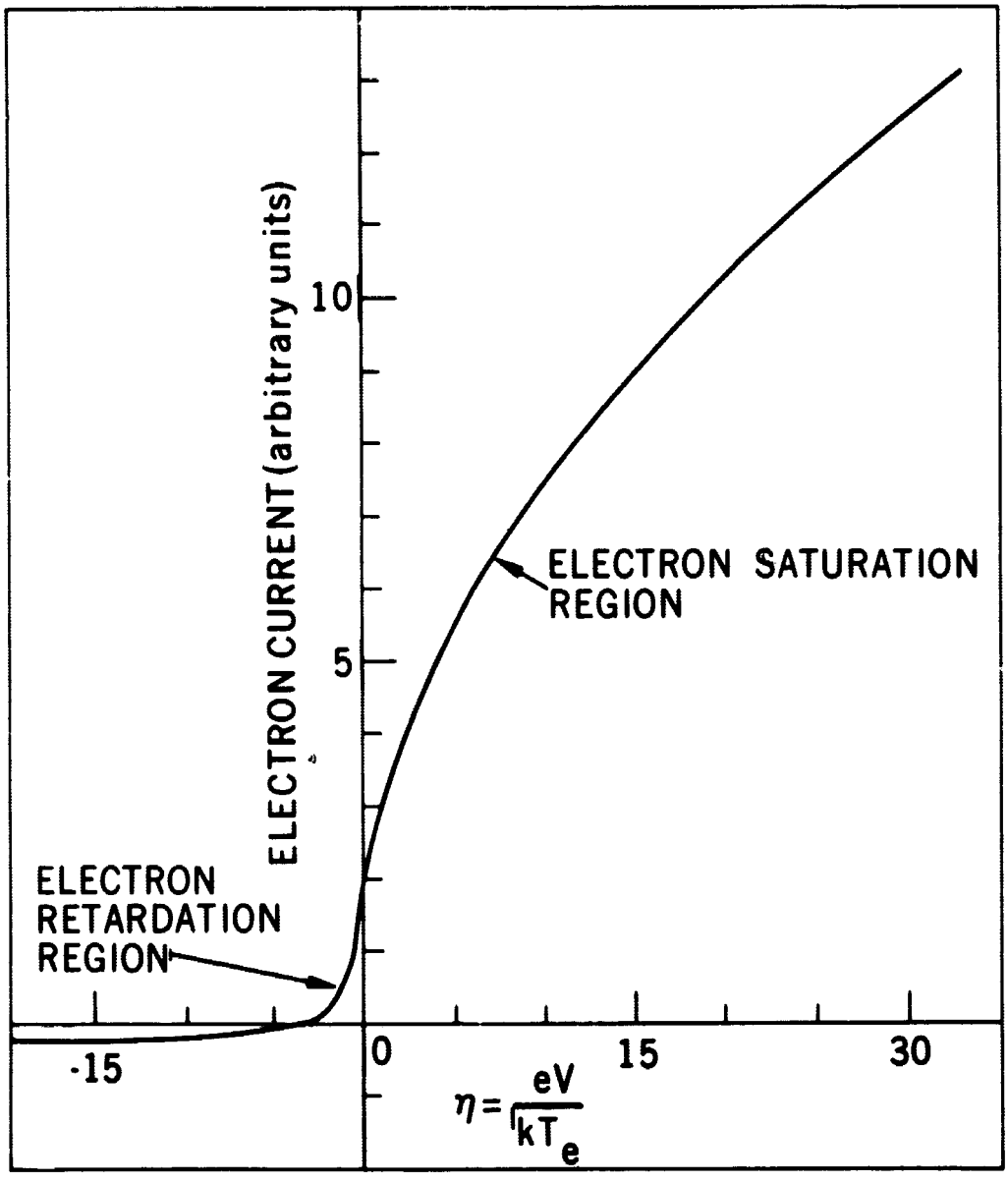

Figure 10–Theoretical volt-ampere characteristic

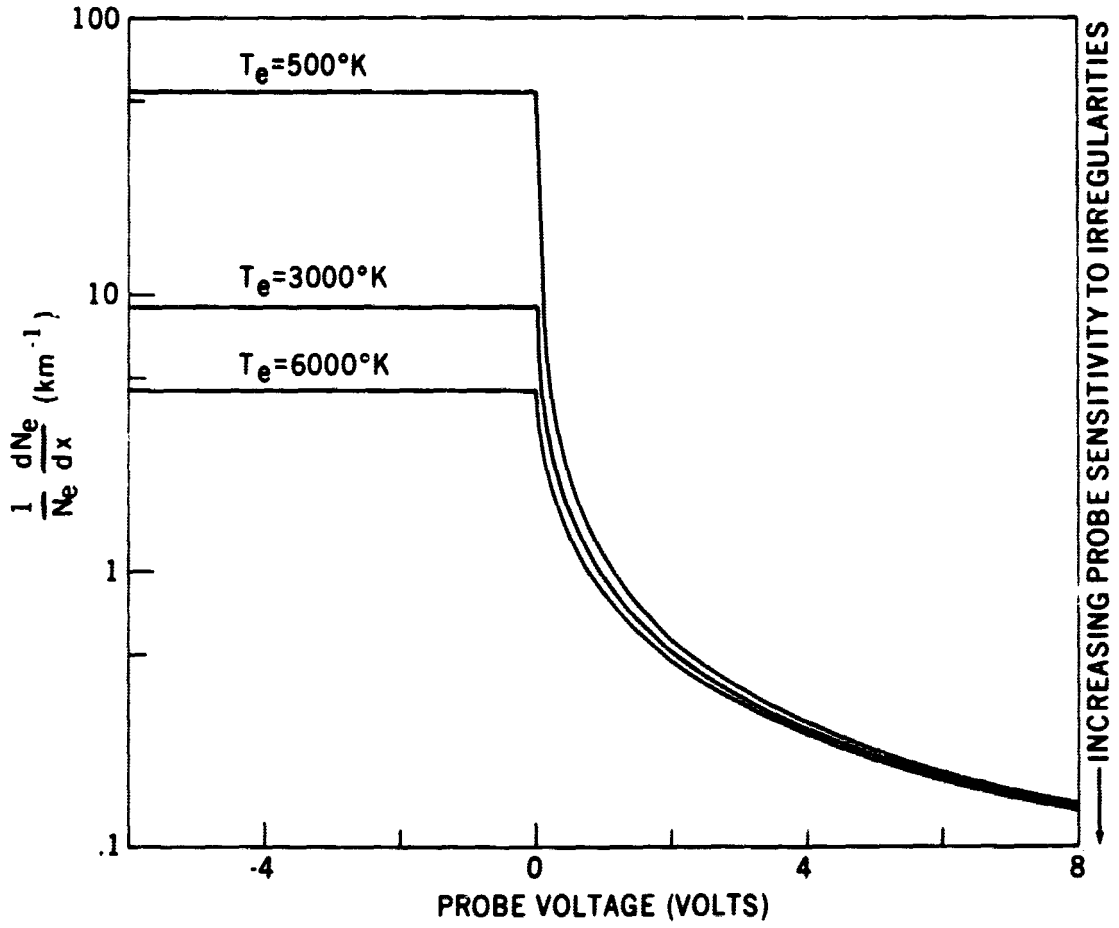

Figure 11a–Minimum electron density gradients required to produce detectable fine structure. N_e gradients are detected more readily in the electron saturation region of the ampere-volt curve

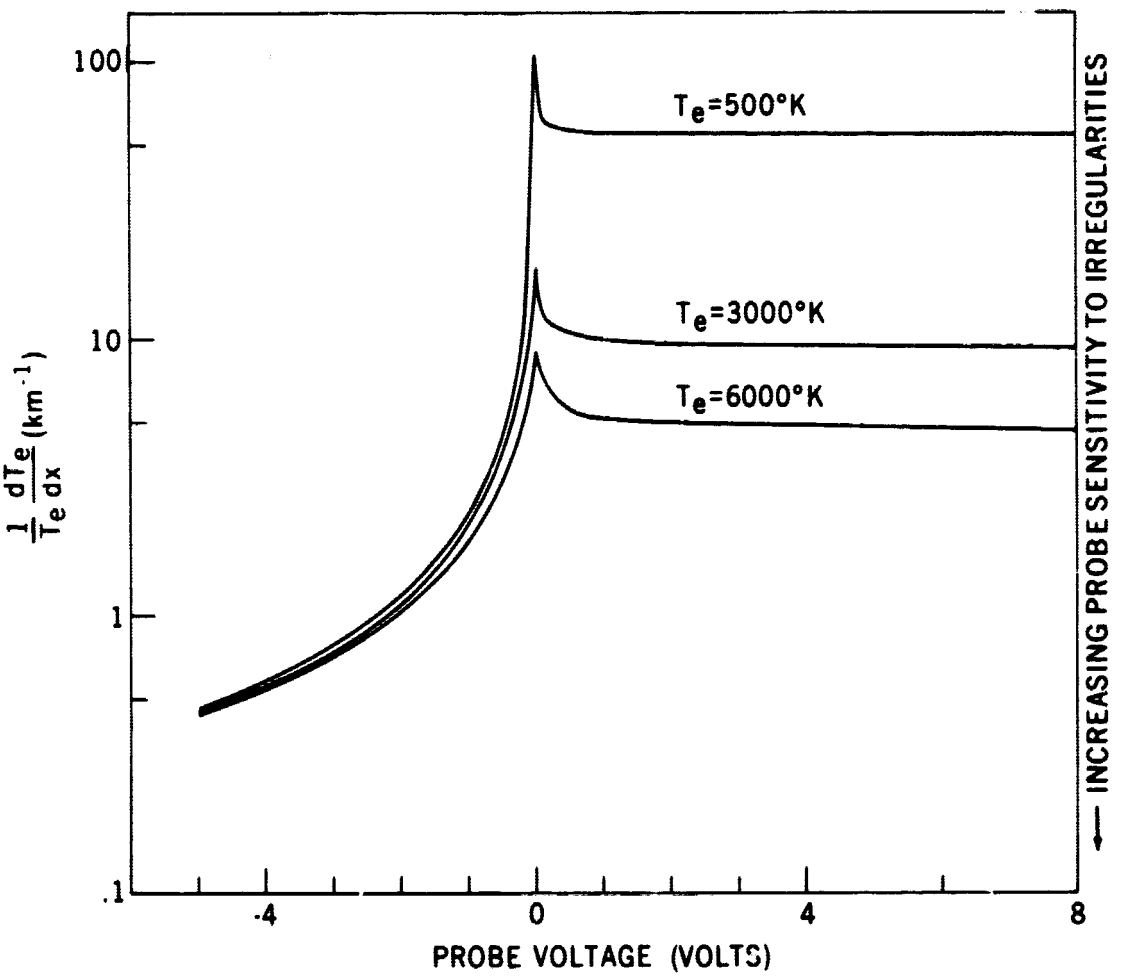

Figure 11b–Minimum electron temperature gradients required to produce detectable fine structure. T_e gradients are dete ed more readily in the electron retardation region of the volt-ampere curve.